Preparation of Hollow Fibers for the Removal of Volatile Organic Compounds from Air

S. DENG, A. TREMBLAY, T. MATSUURA

Industrial Membrane Research Institute, Department of Chemical Engineering, University of Ottawa, Ottawa, Canada, K1N 6N5

Received 7 June 1996; accepted 22 August 1996

ABSTRACT: Hollow-fiber membranes were prepared to remove volatile organic vapors (VOCs) from a nitrogen or air stream. Conditions were found to spin hollow fibers of high performance for the removal of VOCs. The effect of temperature on the permeation of nitrogen gas and acetone vapor was studied. It was found that nitrogen permeation was governed by diffusion while vapor permeation was governed by sorption. There were two distinct mechanisms for vapor permeation, depending on temperature. Performance data for hollow fibers with and without a silicone rubber coating at the internal surface were compared. The effect of the presence of water vapor in the feed was also studied. © 1998 John Wiley & Sons, Inc. J Appl Polym Sci 69: 371–379, 1998

Key words: hollow fiber; hollow fiber module; membrane vapor separation; VOC removal

INTRODUCTION

In recent years, air pollution has become most serious, especially in advanced countries. In these countries, many industrial processes handling organic solvents produce solvent-containing exhaust streams. These streams cause not only severe air pollution problems but also a significant economic loss. From an environmental point of view, it is necessary to limit and control organic vapor emissions because they affect the compositions of the ozone layer, the change of climate, the growth and decay of plants, and the health of human beings and all animals. Two types of conventional organic emission control techniques are still used[1,2]: (1) processes to recover organic vapors, including adsorption, absorption, and condensation, and (2) processes to destroy organic vapors, including direct flame incineration, thermal incineration, and catalytic incineration. Each of these techniques has advantages and disadvantages, in regard to safety, performance, operating costs, and space facilities. In recent decades, a significant achievement was made in many applications of membrane technologies. The separation of organic vapors by a membrane process may have great economic potential.[3,4]

For example, Chmiel et al. reported on a process in which adsorption and membrane separation are coupled to remove volatile organic vapors (VOCs) from exhaust gas.[5] The concentration of a component, (1-methoxy-propyl)acetate, of a solvent in the desorbate stream by a membrane module was demonstrated. The hydrocarbons in stripping air from the soil were adsorbed and then the desorbed vapor was concentrated by a membrane process.[6] Other attempts were also made to explore the possibility of membrane processes to remove VOCs from the air.[3,4,7–12]

Aromatic polyimide (PI) and polyetherimide

Correspondence to: T. Matsuura.

Contract grant sponsors: Institute for Chemical Science and Technology; Natural Sciences and Engineering Council of Canada; Ministry of Education and Training Ontario.

Journal of Applied Polymer Science, Vol. 69, 371–379 (1998)
 CCC 0021-8995/98/020371-09

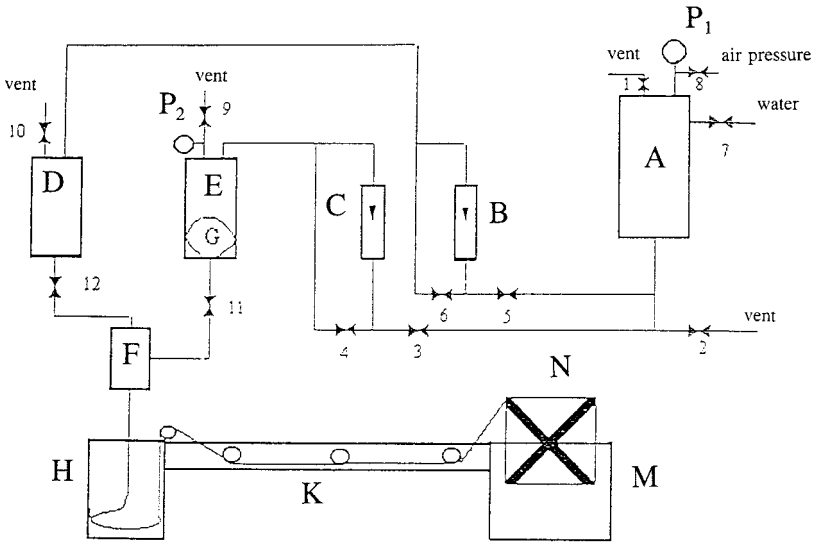

A: Water Reservoir
B,C: Rotameter
D: Internal Coagulant Tank
E: Polymer Solution Tank
F: Spinneret
G: Polymer Solution Bag
H,M: Gelation Tanks
K: Hollow Fiber Leadway
P_1, P_2: Pressure Gauges
1 through 10: Solenoid Valves Controlled by Computer
11,12: Stop Valves

Figure 1 Schematic diagram of hollow-fiber spinning system.

(PEI) were employed for the preparation of membranes to remove various organic vapors from nitrogen by Feng et al.[13,14] and Deng et al.[15] The molecular structure of organic vapors and the selectivity were correlated. A strong correlation was found between the chromatographic retention time of the organic vapors and their selectivity. These experimental results led to a conclusion that sorption is the factor governing the separation of organic compounds from nitrogen. Furthermore, a membrane was prepared by coating the surface of a porous PEI membrane with silicone rubber. The performance of membranes with and without a silicone rubber coating was compared.[16]

The objective of this research was to extend the above investigations to hollow-fiber membranes. Attempts were made to find appropriate conditions to spin hollow fibers of high performance for the removal of organic vapors from nitrogen and air. Hollow fibers were also prepared with and without a silicone rubber coating at the internal wall and their performances were compared. The effect of the presence of water in the feed stream was also studied.

EXPERIMENTAL

Hollow-fiber Spinning

The equipment used to spin hollow fibers is schematically illustrated in Figure 1. It consists of a water reservoir (A), rotameters (B and C), a tank for the internal coagulant (D), a tank for polymer solution (E), a spinneret (F), pressure gauges (P_1 and P_2), gelation baths (H and M), a winding leadway (K), a winding wheel (N), solenoid

valves (1–10) controlled by a computer, and stop valves (11 and 12).

The polymer solution, after being filtered with a 200-mesh filter disk, was loaded into a Teflon bag (G). The bag was then placed in the solution tank (E); the bag opening faced downward. The reservoir (A) was filled with tap water. Then, air pressure was applied to the reservoir (A) and water started to flow to the tanks (D) and (E) through valves 4 and 6. It was important to vent the air inside the tanks (D) and (E) by opening valves 9 and 10 at this stage. When both tanks were filled, valves 4, 6, 9, and 10 were closed and valves 11 and 12 were opened. The internal coagulant (water) and polymer solution flew from the tank (D) and the Teflon bag (G) in the tank (E), respectively, and the flow rates were measured by rotameters (B) and (C). The flow rates were controlled by needle valves attached to the rotameters. The polymer-solution pressure was measured by the pressure gauge (P_2). The internal coagulant from the tank (D) flew through the internal tube of the spinneret while the polymer solution flew through the annular space between the internal tube and the spinneret wall. The polymer solution, after passing through an air gap, entered the first gelation bath (H) that was filled with the external coagulant (water). Then, the fiber was guided through the winding leadway (K) under three pulleys. Finally, the fiber was wound around a winding wheel (N) that was driven by a motor. When an internal coagulant other than water was used, the tank (D) was disconnected from the reservoir (A) and the coagulant fluid flew from the tank (D) through the internal tube of the spinneret under gravitational force.

Fourteen hollow fibers were spun. The details of the fiber-spinning conditions are given in Table I. From hollow fibers 1–5, the PEI concentration increased progressively from 25.0 to 30.0 wt %, while the $LiNO_3$ concentration was kept constant at 1.0 wt %. The balance was DMAc solvent. The polymer-solution temperature was increased together with an increase in the polymer concentration, since, otherwise, the polymer solution viscosity became too high. Internal coagulants were either an aqueous glycerol solution or water, whereas the external coagulant was always water. The $LiNO_3$ concentration for hollow fibers 6–9 was 0.5 wt %. The PEI polymer concentration increased progressively from 25.0 to 30.0 wt %. The internal coagulants were either an aqueous glycerol solution or *n*-hexanol. Acetone was added to the polymer solution of

Table I Hollow-fiber Spinning Conditions[a]

	Hollow Fibers													
	1	2	3	4	5	6	7	8	9	10	11	12	13	14
Polymer solution compositions (wt %)														
PEI	25.0	26.5	28.0	30.0	30.0	25.0	26.5	28.0	30.0	24.1	25.6	27.0	29.0	20.0
$LiNO_3$	1.0	1.0	1.0	1.0	1.0	0.5	0.5	0.5	0.5	1.0	1.0	1.0	1.0	1.0
DMAc	74.0	72.5	71.0	69.0	69.0	74.5	73.0	71.5	69.5	71.3	70.0	68.6	66.7	79.0
Acetone	0.0	0.0	0.0	0.0	0.0	0.0	0.0	0.0	0.0	3.6	3.5	3.4	3.3	
Polymer solution temperature (°C)	23	23	25	26	30	23	24	25	26	24	25	30	26	25
Internal coagulant[b]	glyc	glyc	water	glyc	glyc	glyc	C_6OH	glyc	glyc	water	glyc	water	glyc	glyc

[a] Pressure applied to polymer solution, 20 psig except hollow fiber 5 (40 psig); air gap, 80 cm; temperature of internal coagulant, 23°C; flow rate of internal coagulant, 7.5–9.2 mL/min; gelation bath temperature, 16–19°C.

[b] glyc = 25% (v/v) aqueous glycerol solution; C_6OH = *n*-hexanol.

hollow fibers 10–13. $LiNO_3$ concentration was maintained at 1.0 wt %. Internal coagulants were either water or an aqueous glycerol solution. Hollow fiber 14 was spun for surface coating with silicone rubber. This hollow fiber is very porous due to the low (20 wt %) polymer concentration of the spinning solution.

Treatment of Hollow Fibers

After gelation, hollow fibers were immersed in a water bath for 2 days in order to discharge the solvent in fibers completely. The hollow fibers were then subjected to a leak test. For this purpose, nitrogen gas at 20 psig was introduced to the bore side of the hollow fiber from one end while the other end was closed. Pinholes on the hollow-fiber surface were detected by gas bubbles released from pinholes to the water bath. Fibers with pinholes were discarded and pinhole-free fibers were shrunk in a hot water bath of 85°C for 10 min before they were subjected to solvent exchange.

Two solvents were used for the purpose of solvent exchange: One was ethyl alcohol and the other was a 50% aqueous glycerol solution. The water wet hollow fibers were immersed in one of the solvents for 2 days to replace water with the solvent. The hollow fibers were then dried in ambient air for a couple of days. The dimensions of the hollow fibers were determined after drying and the results summarized in Table II. Ethanol was used to exchange the solvent of hollow fiber 14; therefore, the hollow fiber is hereafter called hollow fiber 14E.

Table II Hollow-fiber Dimensions

Hollow Fibers[a]	i.d. (mm)	o.d. (mm)	Wall Thickness (mm)
1E	0.708	1.183	0.238
2E	0.754	1.237	0.242
3E	0.667	1.218	0.276
4E	0.725	1.206	0.241
5E	0.650	1.206	0.278
1G	0.719	1.177	0.229
2G	0.766	1.264	0.249
3G	0.676	1.234	0.279
4G	0.760	1.247	0.244
6E	0.719	1.183	0.232
7E	0.754	1.114	0.180
8E	0.731	1.230	0.250
9E	0.719	1.235	0.258
6G	0.719	1.241	0.261
7G	0.754	1.137	0.192
8G	0.754	1.276	0.261
9G	0.795	1.270	0.238
10E	0.632	1.253	0.310
11E	0.731	1.206	0.238
12E	0.731	1.268	0.269
13E	0.626	1.114	0.244
14E	0.706	0.996	0.145
10G	0.742	1.183	0.221
11G	0.766	1.288	0.261
12G	0.746	1.286	0.270
13G	0.738	1.247	0.255

[a] E, ethyl alcohol, was used for solvent exchange. G, aqueous glycerol solution, was used for solvent exchange.

Silicone Rubber Coating

The bore side of hollow fiber 14 was coated with silicone rubber. Silgard 184 silicone elastomer and its curing agent, supplied by Dow Corning Corp., were used. The bore side of the dried hollow fiber was first washed with ethanol. A silicone rubber solution was then injected to the bore side of the hollow fiber and left there for about 10 min. After draining the ethanol for 10–15 min, air was forced into the fiber under pressure for about 3 h to dry the silicone rubber layer. The coating was repeated four times.

Hollow Fiber Bundle Preparation

Hollow fibers were cut to a length of 30 cm and 20 fibers were collected into a bundle. Epoxy glue was applied on both ends of the bundle, each end potted into a polypropylene tube of 8 cm in length. After 4 h of epoxy curing, the bundle was transferred to a stainless-steel cylinder specially designed for the permeation experiment, before the cylinder (permeation cell) was connected to a vapor permeation test unit (Fig. 2). The feed vapor was introduced into the bore side of the hollow fiber, while the permeate was collected on the shell side. The total membrane area (bore side) in a module was from 130 to 180 cm^2.

Permeation Experiments

Before starting the permeation experiments, a vacuum was applied on the shell side of the hollow fiber for 4 h to remove any residual solvent. A mixture of a chosen organic vapor and nitro-

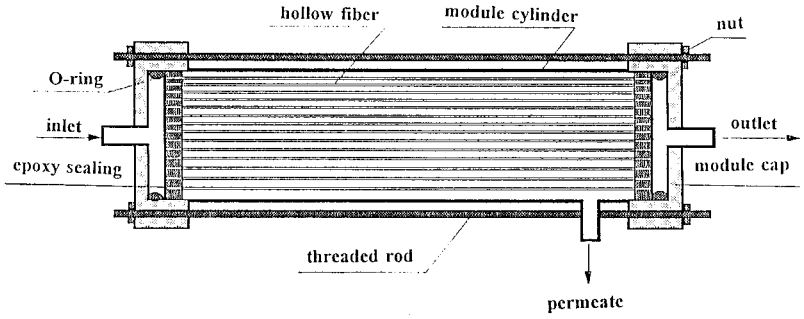

Figure 2 Schematic representation of hollow-fiber module.

gen was then introduced to the bore side as feed. The vapor/nitrogen mixture was produced in a saturator where the feed nitrogen gas stream was saturated with organic vapor while nitrogen gas bubbles were passing through the organic liquid. The temperature of the saturator was maintained between 15 and 17°C. The flow rate of the feed stream was 70–120 mL/min. The permeation cell was housed in an isothermal chamber whose temperature could be controlled within ±0.5°C. The permeate side of the permeation cell was connected to two cold traps immersed in liquid nitrogen, which were followed by a Duoseal vacuum pump (Model 400). The pressure on the permeate side was maintained below 665 Pa (5 mmHg). The feed gas stream was connected to a Varian Gas chromatograph (Model 3400) both at the inlet and at the outlet of the feed chamber of the permeation cell through bypass valves to determine the composition of the feed mixtures.

The permeation rate of pure nitrogen was determined in the following way: A bubble flow meter was connected to the feed chamber outlet of the permeation cell and the inlet valve was closed as illustrated in Figure 3. When the permeate side of the permeation cell was evacuated by a vacuum pump, the nitrogen in the feed chamber was sucked through the membrane, drawing the soap film in the burette of the bubble flowmeter downward. The permeance of pure nitrogen gas through the membrane, J_N (mol $s^{-1}m^{-2}Pa^{-1}$), was obtained by the following relationship:

$$J_N = \frac{1}{6 \times 10^7} \frac{VP_1}{ART(P_1 - P_3)} \quad (1)$$

where V is the volumetric permeation rate (mL/min) of nitrogen through the membrane measured by the bubble flowmeter, A; the effective membrane area (m^2); T, the absolute temperature (K); P_1, the feed pressure (Pa); P_3, the downstream pressure (Pa); and R, a gas constant, 8.314 (J/K Pa).

Assuming that the permeance of nitrogen, J_N, is unaffected by the presence of an organic vapor, which was confirmed by our earlier work,[14] the organic vapor permeance (mol $s^{-1}m^{-2}Pa^{-1}$) is obtained by solving the following set of equations:

$$Q_N = J_N[P_1(1 - \sum Y_{i,1}) - P_3(1 - \sum Y_{i,3})] \quad (2)$$

$$Q_i = J_i[(P_1Y_{i,1}) - (P_3Y_{i,3})] \quad (3)$$

$$Y_{i,3} = \frac{Q_i}{\sum Q_i + Q_N} \quad (4)$$

where the Q's are permeation fluxes (mol s^{-1} m^{-2}); the P's, pressures (Pa); and Y's, the mol fractions of the organic vapor; the subscripts N and i represent nitrogen gas and organic vapor, respectively, and subscripts 1 and 3 represent the

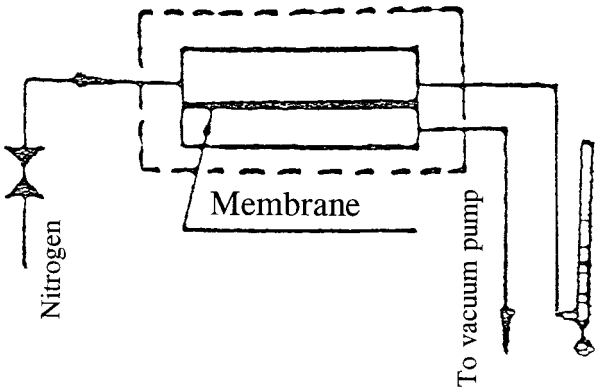

Figure 3 Schematic diagram of the system of the measurement of nitrogen and air-permeation rates.

Table III Results of Hollow-fiber Permeation Experiments at 24°C

Hollow Fibers	Hollow Fiber Area (cm^2)	$J_N \times 10^9$ (mol s^{-1} m^{-2} Pa^{-1})	$J_a \times 10^9$	J_a/J_N
1E	127.2	14.2	16.1	1.13
2E	133.9	1.05	16.1	15.4
3E	115.2	56.3	24.8	0.44
4E	124.2	0.00884	1.74	196.7
5E	94.7	0.0957	1.73	18.1
1G	134.7	0.0135	3.95	292.6
2G	123.4	0.00384	3.81	992.2
3G	111.9	0.293	1.68	5.73
4G	130.6	0.00032	2.00	6250
6E	133.8	29.4	24.5	0.833
7E	153.7	0.622	0.688	1.11
8E	126.0	2.20	17.9	8.14
9E	126.5	0.133	2.97	22.3
6G	133.3	0.161	4.02	25.0
7G	132.7	0.520	1.51	2.90
8G	130.1	—	2.19	—
9G	140.6	0.00476	3.24	680.7
10E	123.1	35.9	18.1	0.504
11E	149.2	0.635	17.1	26.9
12E	133.2	20.9	30.5	1.46
13E	126.0	0.152	4.34	28.6
10G	139.9	0.0502	1.67	33.3
11G	159.2	0.0878	2.31	26.3
12G	137.8	0.0640	1.74	27.2
13G	129.4	0.00078	3.39	4346

feed and the permeate, respectively. Considering eqs. (2)–(4), Q_i, P_1, P_3, $Y_{i,1}$, and J_N are quantities known from the permeation experiments. Consequently, the three unknowns, J_i, Q_N, and $Y_{i,3}$, can be calculated from the above three equations.

RESULTS AND DISCUSSION

The results of the nitrogen and acetone vapor permeation experiments are summarized in Table III. Combined with the spinning conditions given in Table I, the following tendencies can be found for the effect of hollow-fiber spinning on hollow-fiber performance:

1. Comparing the lowest and highest PEI concentration in each group, that is, 1E and 5E, 1G and 4G, 6E and 9E, 6G and 9G, 10E and 13E, and 10G and 13G, both J_N and J_a (acetone permeance) were smaller and the ratio J_a/J_N was higher at higher PEI concentration, except when 10G and 13G were compared.
2. Comparing the two solvents used for the solvent exchange, the aqueous glycerol solution resulted in higher J_a/J_N ratios with only one exception of hollow fiber 11.
3. While the J_N values changed in a range 3.20×10^{-13} to 5.63×10^{-8} mol s^{-1} m^{-2} Pa^{-1}, the J_a values changed in a range 6.9×10^{-10} to 3.05×10^{-8} mol s^{-1} m^{-2} Pa^{-1}. The change in nitrogen permeance was much more than was the change in the acetone vapor permeance.
4. A decrease in the amount of $LiNO_3$ in the casting solution decreased the J_a/J_N ratio

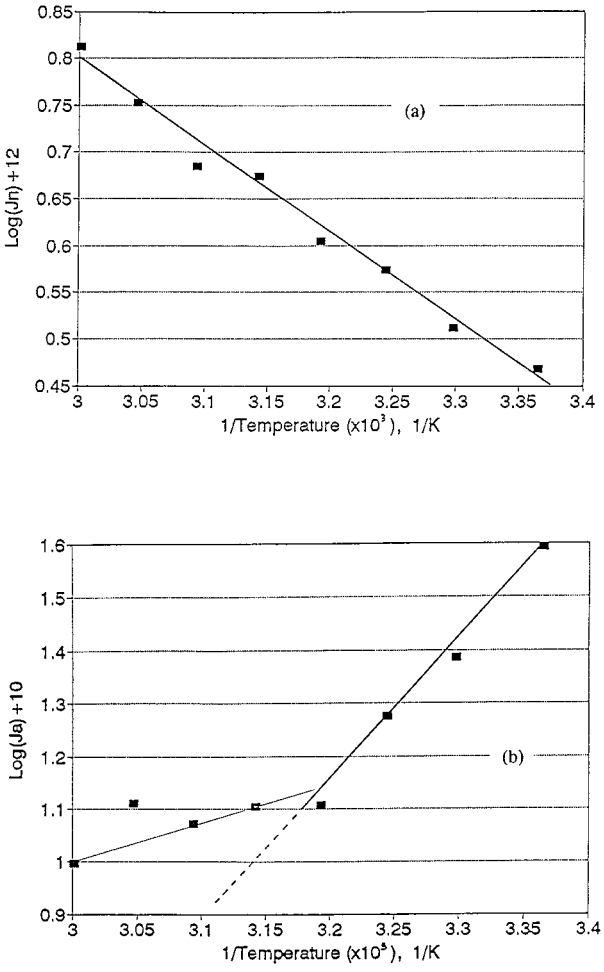

Figure 4 Temperature effect for the permeation of (a) nitrogen and (b) acetone.

Table IV Effect of the No. Silicone Layers on Nitrogen Permeance at 24°C

No. Coated Layers	$J_N \times 10^9$ (mol s^{-1} m^{-2} Pa^{-1})
0	—
1	2.27
2	1.00
3	0.655
4	0.158

Silicone rubber coating was applied on hollow fiber 14E.

with only one exception of the comparison between 3E and 8E.

Hollow fiber 4G was used to study the temperature effect on the hollow-fiber permeation. J_N and J_a were obtained at different temperatures and subjected to an Arrhenius plot as illustrated in Figure 4. While J_N showed a linear relationship over the entire range of temperature studied, corresponding to an activation energy of 17.9 kJ/mol, the plot of J_a showed a clear inflection point at $1/T = 0.00319$ (40°C). Activation energies of −14.65 and −55.7 kJ/mol, respectively, were found valid at the higher- and lower-temperature range. These results indicate that (1) the membrane transport of nitrogen and that of acetone vapor are governed by different mechanisms—diffusion is governing the nitrogen transport, while sorption is governing the acetone transport; and (2) there are two different mechanisms governing the transport of acetone vapor—one at temperatures above 40°C and the other below 40°C.

Table V Comparison of Permeance Data for PEI Membranes with (14E-5) and Without (13G) Silicone Rubber Coating

	Permeance × 10^9 (mol s^{-1} m^{-2} Pa^{-1})	
Vapors	Membrane 14E-5	Membrane 13G
Pentane	1740	29
Benzene	1070	268
Dioxane	980	367
Methanol	3580	4170
Ethanol	2570	1440
Acetone	1680	122
Methyl acetate	1820	174
Water	8280	6580

Table VI Comparison of Experimental Results Between Nitrogen and Air-feed Streams

	Permeance × 10^9 (mol s^{-1} m^{-2} Pa^{-1})	
Feed Stream	Nitrogen	Air
Nitrogen	0.158	
Air		0.215
Acetone	16.8	21.4
Water	82.8	93.8
Acetone selectivity[a]	106.6	99.3
Water selectivity[a]	524.5	436.3

Membrane, hollow fiber 14E-5; temperature, 24°C.
[a] Selectivity is defined as vapor permeance/nitrogen or air permeance.

The two different mechanisms of acetone vapor transport can be understood in the following way: When the temperature is above 40°C, the acetone vapor permeates through the membrane by the surface flow mechanism, where the layer of acetone adsorbed on the capillary pore wall flows under the pressure gradient. When the temperature is below 40°C, on the other hand, the capillary pore is filled with the acetone vapor by condensation and condensed acetone flows under the pressure gradient. Then, the radius of the pore, r, in which the condensation of acetone takes place at 40°C can be calculated by the following equation:

$$\ln \frac{p}{p_0} = \frac{2\sigma}{\gamma} \frac{M}{\rho RT}$$

where p and p_0 are the partial pressure and saturation vapor pressure of acetone (Pa), respectively; σ, M, and ρ are the surface tension (N/m), molecular weight, and density (m^3/kg) of acetone, respectively; R is a gas constant; and T is the absolute temperature.

Using the following numerical values: p = 15,200 Pa [114 mmHg = saturation vapor pressure of acetone at the temperature (17°C) of the saturator], p_0 = 53,329 Pa (400 mmHg = saturation vapour pressure of acetone at 40°C), $\sigma = 22 \times 10^{-3}$ N/m, ρ = 796 kg/m^3, M = 58.08 kg/kmol, $R = 8.314 \times 10^3$ J/kmol K, and T = 313.2 K, r is calculated to be 9.82×10^{-10} m. This pore size seems to be too large for vapor-separation membranes.

Table VII Comparison of Membrane 14E-5 (with Silicone Rubber Coating) and Membrane 4G (Without Silicone Rubber Coating) for the Separation of the Feed Mixtures of Air/Acetone/Water at 24°C

	Membrane 14E-5		Membrane 4G	
	In Feed	In Permeate	In Feed	In Permeate
	(Mol Fraction)			
Air	0.848	0.069	0.841	0.004
Acetone	0.141	0.833	0.147	0.029
Water	0.011	0.098	0.012	0.967

Nitrogen permeance was measured after coating hollow fiber 14E different times. The results given in Table IV show that the permeance decreases with the number of coatings. The hollow fiber coated with silicone rubber four times is hereafter called hollow fiber 14E-5.

Table V compares the permeance data obtained for a silicone rubber-coated membrane (14E-5) and those obtained for a membrane without the silicone rubber coating (13G). The silicone-coated membrane is featured by a narrower range of vapor permeance as compared with the membrane without the silicone rubber coating. For example, the water permeance of membrane 14E-5 is 8280×10^{-9} mol s^{-1} m^{-2} Pa^{-1} and is 4.8 times greater than the permeance of pentane, whereas the water permeance of the 13G membrane is 6580×10^{-9} mol s^{-1} m^{-2} Pa^{-1} and is 227 times greater than the permeance of pentane. Since the water permeances are not very different, the above data indicate that silicone coating enhances the permeation of hydrophobic hydrocarbon molecules.

Table VI compares the permeance data of acetone and water in the presence of nitrogen and air in feed streams. Membrane 14E-5 with the silicone rubber coating was used for the experiment. Both acetone and water permeances increased from nitrogen to air; however, selectivities decreased.

Table VII shows the results of permeation experiments for feed mixtures of air/acetone/water. The experiments were carried out with both membrane 14E-5 (silicone rubber-coated) and membrane 4G (uncoated). The feed and permeate compositions are reported in the table. The table shows that acetone vapor was dominant in the permeate of membrane 14E-5, while water vapor was dominant in the permeate of membrane 4G. These results are explained by the relatively hydrophobic nature of membrane 14E-5 and the relatively hydrophilic nature of membrane 4G.

CONCLUSIONS

The following conclusions can be drawn from the above experimental results:

1. Nitrogen permeance of hollow fibers prepared under different spinning conditions covers a wide range, while acetone permeance covers a much narrower range of variation.
2. Nitrogen permeation is governed by diffusion, whereas acetone permeation is governed by sorption.
3. There are two different mechanisms of acetone vapor permeation, depending on the temperature.
4. The range of variation in permeance for different vapors is narrowed by the silicone coating.
5. The selectivity for vapor/gas separation is lowered when the feed gas stream is changed from nitrogen to air.
6. With a feed mixture containing both acetone and water, the permeate vapor is dominated by acetone when a silicone-coated hydrophobic membrane is used, whereas the permeate vapor is dominated by water when a PEI membrane without the silicone coating is used.

Financial support by the Institute for Chemical Science and Technology, the Natural Sciences and Engineering Council of Canada (IOR Grant), and the Ministry of Education and Training Ontario (URIF Grant) to this project are gratefully acknowledged.

REFERENCES

1. K. Wark and C. F. Warner, *Air Pollution: Its Origin and Control,* Harper & Row, New York, 1986.
2. L. Theodore and A. J. Buonicore, *Air Pollution Control Equipment,* Vol. 2, *Gasses,* CRC Press, Boca Raton, 1988.
3. R. D. Behling, in *Proceedings of 6th Annual Mem-*

brane Technology Planning Conference, Cambridge, 1986, Session V-4.
4. R. W. Baker, N. Yoshioka, J. M. Mohr, and A. J. Khan, *J. Membr. Sci.,* **31,** 259 (1987).
5. H. Chmiel, V. Mavrov, and M. Kaschek, in *Environmental Aspects in Materials Research,* H. Warlimont, Ed., DGM Informationsgesellschaft Verlag, 1994, pp. 275–282.
6. H. Chmiel, V. Marvov, and A. Fahnrich, in *Proceedings at the 1995 Thirteenth Annual Membrane Technology / Separations Planning Conference,* Newton, MA, Oct. 23–25, 1995.
7. K. V. Peinemann, J. M. Mohr, and R. W. Baker, in *Recent Advances in Separation Technologies - III,* AIChE Symposium Series 250, Vol., 82, 1986, p. 19.
8. K. Kimmerle, C. M. Bell, W. Gudernatsch, and H. Chmiel, *J. Membr. Sci.,* **36,** 577 (1988).
9. H. Paul, C. Philipsen, F. J. Gerner, and H. Strathmann, *J. Membr. Sci.,* **36,** 363 (1988).
10. I. Pinnau, J. G. Wijmans, I. Blume, T. Kuroda, and K. V. Peinemann, *J. Membr. Sci.,* **37,** 81 (1988).
11. F. W. Billmeyer, Jr., *Textbook of Polymer Science,* 3rd ed., Wiley, New York, 1984.
12. O. M. Ilinitch, C. L. Semin, M. V. Chertova, and K. I. Zamaraev, *J. Membr. Sci.,* **66,** 1 (1992).
13. X. Feng, S. Sourirajan, H. Tezel, and T. Matsuura, *J. Appl. Polym. Sci.,* **43,** 1071 (1991).
14. X. Feng, S. Sourirajan, H. Tezel, and T. Matsuura, *Ind. Eng. Chem. Res.,* **32,** 533 (1993).
15. S. Deng, S. Sourirajan, T. Matsuura, and B. A. Farnand, in *Sixth International Conference on Pervaporation Processes in the Chemical Industry,* Ottawa, Sept. 27–30, 1992.
16. S. Deng, K. Lang, J. Wang, A. Tremblay, and T. Matsuura, *Membr. J. Kor.,* **7,** 22 (1997).